A DESIGN OF EXPERIMENT FOR EVALUATING INSTALLATION EFFECTS AND THE INFLUENCE OF BLADE LOADING ON THE AEROACOUSTICS OF AN AUTOMOTIVE ENGINE COOLING FAN

Elias TANNOURY[1], Bruno DEMORY[1], Manuel HENNER[1], Pierre-Alain BONNET[1], Patrice CAULE[2], Yoann CRETEUR[2]

[1] *Valeo Thermal Systems, Fan system simulation department, 8 rue Louis Lormand, 78321 La Verrière, France*

[2] *Technofan- SAFRAN group, 10 place Marcel Dassault, BP 53, 31702 Blagnac, France*

SUMMARY

A design of experiment for assessing the influence of blade loading and fan integration on the emitted noise from an automotive engine cooling fan is carried out. Three fans delivering the same pressure rise at the target operating point are designed by the means of CFD. The blades' designs are different: the first one has relatively large chord lengths combined with high stagger angles at the hub while the second one has small chord lengths and stagger angles at the hub, and the third one is designed to operate at lower rotational speed. 17 fan supports with various geometrical parameters are designed and manufactured according to a Nearly Orthogonal Latin Hypercube Design of Experiment. Each fan is tested with all the supports at several operating points in an anechoic chamber. The results and the impact of each parameter on the tonal, broadband and total noise are discussed.

INTRODUCTION

Aeroacoustic performances of cooling fans in automotive industry have become a quality factor [1]. However, tighter packaging and the quest for higher performance have made it more difficult to create quieter fans. Consequently, the fan's integration in its environment has acquired a major impact on both its aerodynamic and aeroacoustic performances. Furthermore, depending on the blade's load distribution, the fan is more or less sensitive to its environment. A design of experiment (DOE) is carried out to assess the influence of various, commonly encountered geometrical parameters on the aeroacoustics of such cooling fans. The goal of the DOE is to maximize the information gained from the experiment while keeping the cost at minimum.

The work is conducted in two phases, the first one being a specific study on blade loading, and the second one being a specific study on the fan's interaction with its support:

- 3 fans delivering the same pressure rise at the target operating point are designed and simulated numerically. The first blade is more loaded near the bottom, whereas the second has greater load near the tip, and the third is designed to operate at lower rotational speed. The fans are denoted Fan A, Fan B and Fan C respectively. The differences between the geometries of the blades are shown in Figures 1 and 2.

Figure 1 - Left to right: Front view of Fan A, Fan B and Fan C.

Figure 2 – Left to right: Leading edge of Fan A, Fan B and Fan C.

- 17 supports are designed according to a Nearly Orthogonal Latin Hypercube (NOLH) design of experiment [2] based on one physical parameter (flow rate) and 6 geometrical ones. They include the rotor-strut distance, the strut's sweep angle, the strut's aspect ratio, the tip clearance and the rotating ring's immersion in the shroud. Three examples of fan supports are shown in Figure 3.

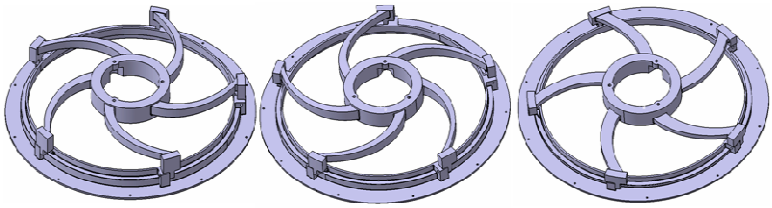

Figure 3 - Examples of supports with various geometrical parameters

The fans and the supports are manufactured and tested in an anechoic chamber equipped with a flow-rate control rig. Each of the fans is tested with all the supports at the design point and several other flow rates. This makes a total of 3 designs of experiment, each corresponding to a specific type of blade loading. The results are used to construct a response surface model (RSM) for efficiency and overall noise.

FAN DESIGN

Comparison of fan noise levels is only relevant at the same operating point. Thus, three fans providing the same pressure rise at the target operating point with different blade loading are designed. They are obtained via an optimization loop based on numerical simulations coupled with the optimizer I-Sight. Fans A and B have different stagger angles and chord lengths, that is, Fan A has large chord lengths and stagger angles at the hub compared to small ones for Fan B. Fan C has an additional parameter which is the rotational speed: it is designed to deliver 210 Pa at 2300m^3/h

and 2000 Rpm, compared to 2400 Rpm for fans A and B. Steady Reynolds-Averaged Naviers Stocks (RANS) simulations of the fans are carried out to investigate the load distributions and ensure an equal pressure rise at the target operating point. They are performed using the Star-CCM+ 6.02.009 segregated solver with a two-equation K-ω SST model for turbulence [3]. The predicted and experimental pressure rises are compared at the target operating point in Table 1. Furthermore, the complete pressure rise curves acquired experimentally are plotted in Figure 4.

Table 1 – Static pressure rise (Pa) of Fans A, B and C.

	Fan A (2400 Rpm)	Fan B (2400 Rpm)	Fan C (2050 Rpm)
Experimental	187	184	194
Steady RANS	174	171	166

Experimentally, the fans are almost equivalent at the target operating point of 2300 m^3/h. Below 2200 m^3/h and above 2600 m^3/h, the fans' behaviors are different, with Fan A providing greater pressure rise at low flow rates, and lower pressure rise at high flow rates.

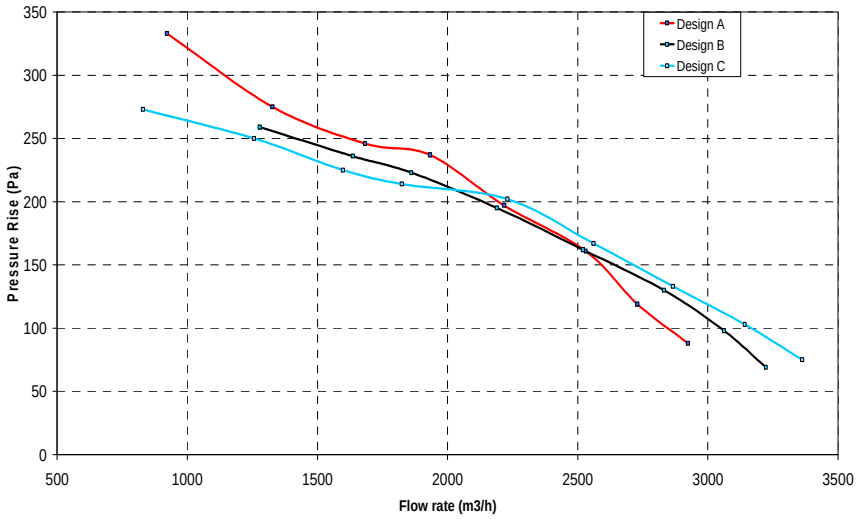

Figure 4 - Experimental pressure rise curves of Fans A, B and C

The zero pressure points are not measured experimentally. Nevertheless, by extrapolating the plots in Figure 4, the zero-pressure points of fans B and C occur at higher flow rates than for Fan A.

Next, total pressure rise profiles are computed to allow an estimation of the blade's loading. They are extracted on a plane downstream of the fan and are shown in Figure 5 as a function of the blade's span. Fan A provides most of its total pressure rise below the blade's mid-span, while fan B starts to generate a significant total pressure rise around the mid-span. Fan C is somewhere in the middle between Fan A and B below 60% of the span, but is the least loaded near the tip. Figure 6 further confirms the trends shown in Figure 5. The maximum total pressure zones are highlighted in yellow and red. Those zones are located between the hub and mid-span for fan A, between the mid-span and the tip for fan B and mostly near the mid-span for fan C.

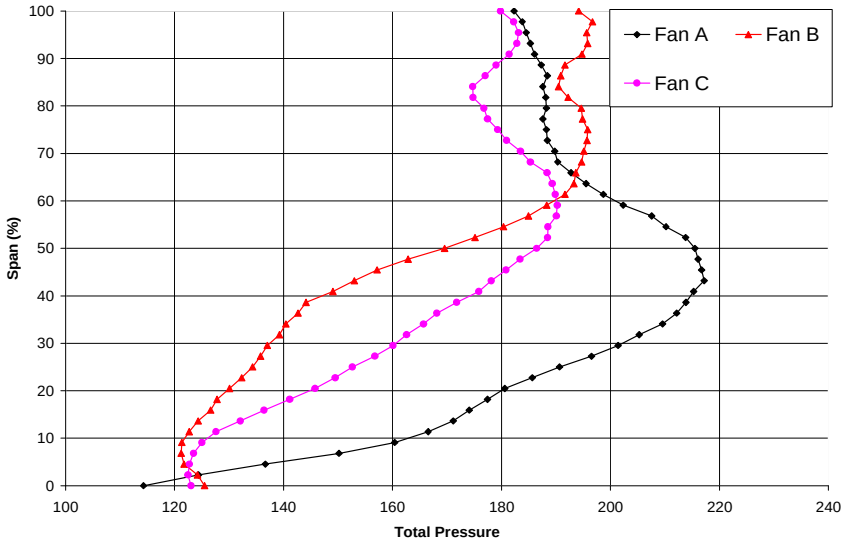

Figure 5 - Total pressure rise vs. blade span

STRUTS DESIGN

The fan's supporting struts are known to have a major influence on both noise and efficiency. In certain contexts and for given operating conditions, they induce a drop in the overall efficiency of the cooling module and an increase in the overall noise level. The extent to which the efficiency drops and the noise increases is defined by the shape of the struts, their distance to the rotor and other geometric parameters such as the tip clearance and the fan's immersion in the shroud.

An experimental DOE is carried out to properly assess the dependence of efficiency and noise on the fan's support design. Six geometrical parameters of the support are selected to conduct the DOE and the mass flow rate is chosen as a seventh parameter to allow controlling the operating point. All the supports have 5 identical struts distributed symmetrically on the azimuth. They are designed to provide mechanical support and not to achieve an aerodynamic function. Thus, they have a rectangular cross-section, and any support can be defined by the following geometric parameters:

- Rotor-strut distance: distance between the rotor's trailing edge, and the strut's leading edge, see Figure 8.

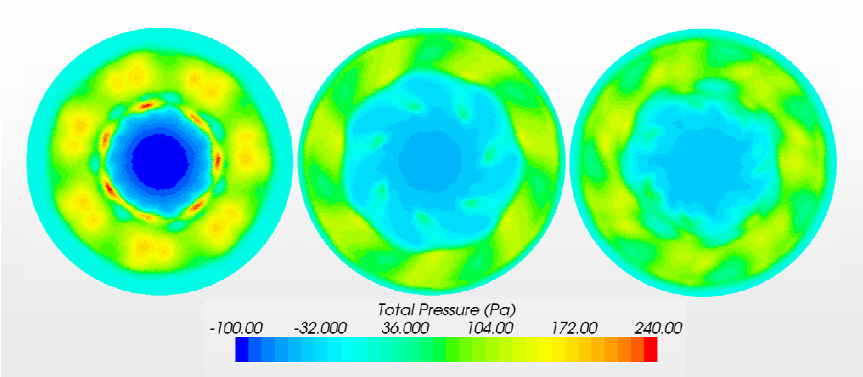

Figure 6 - Total pressure maps downstream of the rotor. Left to right: Fan A, B and C

- Sweep of the struts: angle between the tip of the strut and a radius going through its bottom, see Figure 7.

- Aspect ratio: considered constant along the strut's span, see Figure 7.
- Evolution of the strut's cross-sectional area: it is defined as the ratio between the cross sectional areas of the strut at the bottom and at the tip. A ratio of one means that the strut has a constant cross-sectional area throughout the span, see Figure 8.
- Radial tip clearance: radial distance between the fan's rotating ring and the shroud, see Figure 8.
- Axial tip clearance: or the fan's immersion. It is the axial distance between the rotating ring and the shroud, see Figure 8.

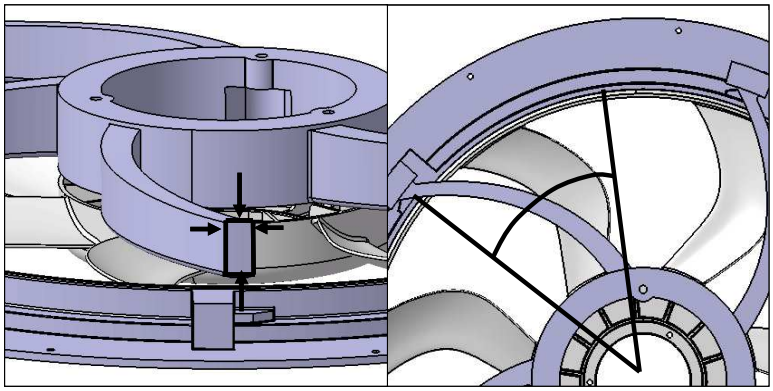

Figure 7 - Left: aspect ratio of the strut.
Right: Sweep of the strut.

A Nearly Orthogonal Latin Hypercube (NOLH) sampling is applied to the distribution of parameters. It allows increasing the number of the examined variables at a fixed number of experiments compared to a Latin Hypercube sampling. However, better space filling is obtained at the expense of orthogonality [2]. In total, 17 designs are generated and manufactured. The combinations of the parameters are shown in Table 2.

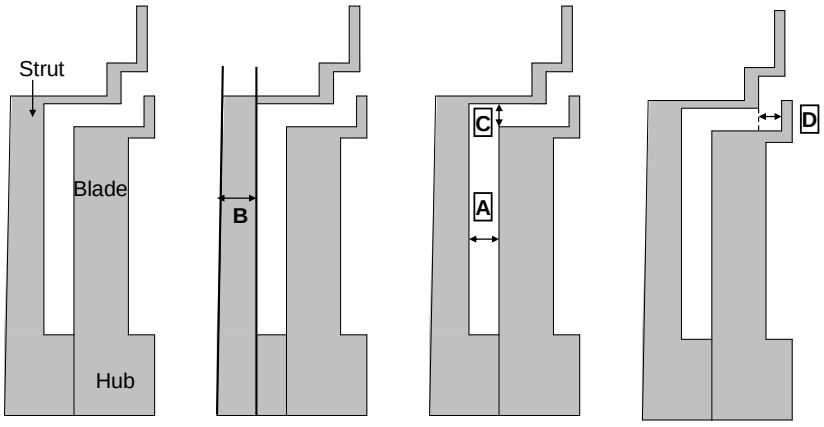

Figure 8 - A: Rotor-strut distance.
B: Evolution of the strut's cross-sectional area.
C: Radial tip clearance.
D: Axial tip clearance.

TESTING AND EXPERIMENTAL CONDITIONS

Noise levels are measured in an anechoic chamber. For this purpose, the fan and its support are mounted at the center of a reverberant panel placed in the middle of the room and ten microphones measure sound pressure levels at the suction side of the fan, see Figure 9. Their locations and the computation of the sound power level are compliant with the ISO standard 3744 [4].

A flow control rig is constructed according to ISO standard DP 5801 and mounted at the back of the reverberant panel. The flow rate is controlled through diaphragms mounted at the plenum's exit downstream of the fan as shown in Figure 9. For a diaphragm diameter D and a measured pressure rise inside the plenum ΔP, the volume flow rate is:

$$Q_v = 0.6 \times \frac{\pi}{4} \times \left(\frac{D}{1000}\right)^2 \times \left(\frac{2 \times \Delta P}{\rho_{air}}\right)^{0.5} \quad (1)$$

Table 2 – NOLH sampling of the design space. The values are percentages of the range of each parameter.

Config.	Flow rate	Rot. - Stat distance	Sweep	Aspect ratio	Evo. section	Radial Tip. Cl.	Axial tip C.
1	31,25	100,00	81,25	37,50	25,12	93,76	56,25
2	6,25	25,00	87,50	56,24	0,00	31,26	62,50
3	12,50	43,75	6,25	25,01	62,56	81,26	100,00
4	18,75	62,50	31,25	100,00	56,28	12,50	75,00
5	75,00	93,75	43,75	12,52	31,16	0,00	81,25
6	100,00	31,25	37,50	81,25	6,28	75,00	87,50
7	62,50	18,75	100,00	31,27	87,44	43,76	93,75
8	56,25	87,50	75,00	93,74	81,40	62,50	68,75
9	50,00	50,00	50,00	50,02	50,00	50,00	50,00
10	68,75	0,00	18,75	62,50	75,12	6,26	43,75
11	93,75	75,00	12,50	43,76	100,00	68,76	37,50
12	87,50	56,25	93,75	74,99	37,44	18,76	0,00
13	81,25	37,50	68,75	0,00	43,72	87,50	25,00
14	25,00	6,25	56,25	87,51	68,84	100,00	18,75
15	0,00	68,75	62,50	18,75	93,72	25,00	12,50
16	37,50	81,25	0,00	68,77	12,56	56,26	6,25
17	43,75	12,50	25,00	6,26	18,84	37,50	31,25

The plenum is made semi-anechoic on the inside by the use of acoustic absorbers to prevent the acoustic waves from traveling upstream. The rotational speed of the fan is maintained constant by varying the voltage and current intensity of the electric motor, thus, the global efficiency of the fan system is computed as follows:

$$\eta = \frac{Q \times \Delta P}{U \times I} \times 100 \quad (2)$$

Q is the volume flow rate (m^3/s), ΔP is the static pressure rise (Pa), U is the voltage (V) between the electric motor's terminals and I is the current intensity running through the motor (A).

Figure 9 - Left: Reverberant panel with fan and microphones.
Center: Flow-rate control rig.
Right: diaphragm for flow-rate control.

Each fan is tested with all seventeen supports and although one operating point is required by the DOE, several flow rates are tested to allow a correct discretization of the pressure rise curve. Examples of different sweep angles, strut thicknesses and aspect ratios are shown in Figure 10. Different immersions are compared in Figure 11, and 204 configurations are tested in total.

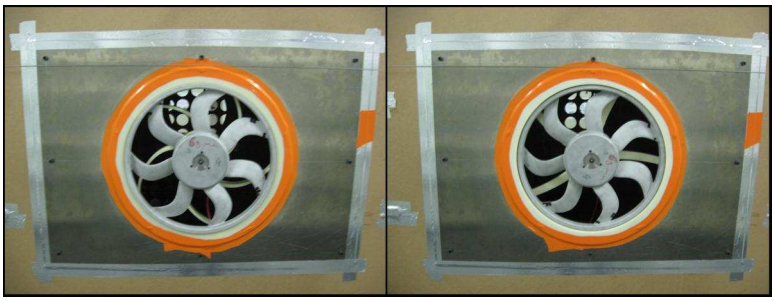

Figure 10 – Front view of Fan C mounted on strut 12 (Left) and strut 5 (Right)

RESULTS OF THE DOE

The analysis of the DOE's results is conducted in two stages: first, comparisons of fan efficiencies and overall noise levels are established, then broadband and tonal noise levels are compared. The first phase of the DOE is achieved by plotting efficiencies and overall Sound Power Levels (SWL) at the target operating point. Consequently, maximum efficiency and minimum noise configurations can be identified. Efficiency and overall SWL are plotted in Figure 12 with an offset by a reference value.

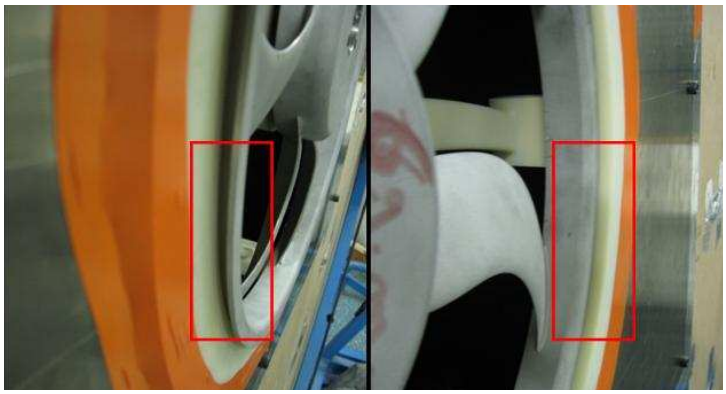

Figure 11 – Close up of the fan that shows the difference in immersion between configuration 12 (Left) and configuration 5 (Right). Left: Emersion, Right: Immersion

First, the efficiencies of the fans are compared. At 2300 m^3/h, Fan C has the highest efficiency followed by Fan A, and then Fan B. However, a fluctuation of efficiency of roughly 6% (maximum) is observed.

From an acoustic point of view, the lower rotational speed of Fan C allows it to be the quietest while fan B is quieter than Fan A on average. Moreover, Fan B is the least sensitive to its environment since an increase (or decrease) of only 1.7 dB(A) is observed depending on the strut's configuration. In contrast, Fan A and Fan C are more sensitive to installation effects: depending on the struts' configuration, a reduction (or increase) in noise level of ≈ 5 dB(A) can be achieved.

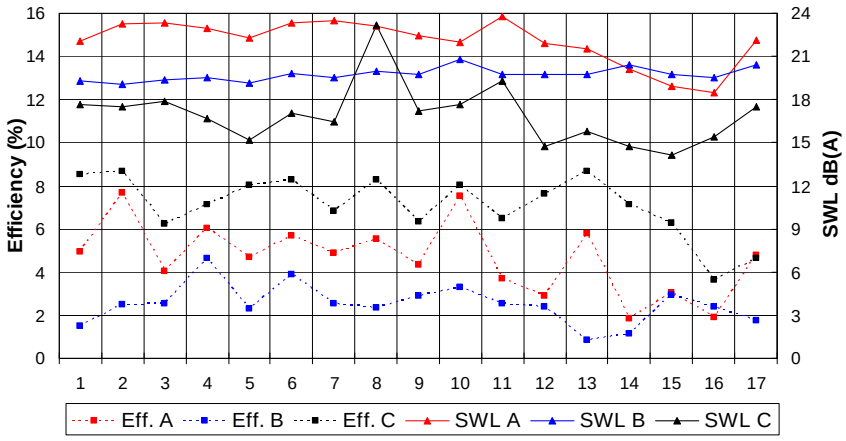

Figure 12 - Efficiencies and Sound power levels of fans A, B and C for each configuration. The scales have been offset by a reference value.

Maximum efficiency and minimum noise are not obtained at the same configuration of struts. Fan C for instance has a maximum efficiency at configuration 13, while minimum noise occurs at configuration 15. Two points of efficiency are traded against 1.5 dB(A). The trend is the same for Fan A with greater amplitude however, since 5 efficiency points are traded against 5 dB(A). The difference between maximum efficiency and minimum noise configurations is less obvious for Fan B since it has relatively flat curves of efficiency and SWL.

In a second stage, the third octave sound spectrum is separated into broadband and tonal noise. The tonal peaks occurring at the blade passing frequency are extracted and summed, thus yielding an overall tonal noise level. A broadband noise level is then computed by summing the rest of the spectrum. Broadband and tonal noise levels of all three fans are shown in Figure 13.

Tonal noise is particularly dependant on the context since a maximum fluctuation of 10 dB(A) is observed. The configurations with small rotor-stator distance are particularly more "tonal" than others. Zero tonal noise configurations are observed for Fan C in the third octave analysis. However, the emergences exist in the narrow band spectrums, but are minimal. By performing a third octave analysis the small tones do not emerge from the broadband spectrum.

Broadband noise is less sensitive to the environment since a maximum fluctuation of 5 dB(A) is observed. Fan B has a particularly low sensitivity to its environment compared to Fans A and C. Its maximum noise level fluctuation is roughly 7 dB(A) for tonal noise and 2 dB(A) for broadband noise.

The difference in behavior of the fans can be attributed to their load distribution. Loading the blade more at the bottom like Fan A or at the mid-span like Fan C allows greater efficiencies. But, it increases the blade's sensitiveness to its environment. Hence, installation effects become more significant. Loading the blade at the tip reduces efficiency in comparison with other types of loadings, but increases the fan's robustness vis-à-vis its environment. The efficiency as well as the sound level become less dependent on the fan's integration in its support.

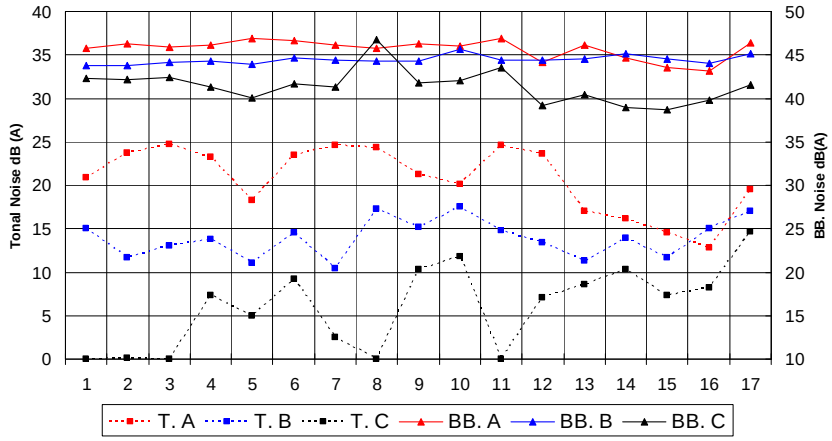

Figure 13 - Tonal and broadband noise of the fans for all the configurations. The scales are offset by a reference value

RESPONSE SURFACE MODEL

The results of all three DOEs are used to create efficiency and overall SWL Response Surface Models (RSM) for each type of blade design. Then, the RSMs are included in an optimization loop created with the optimizer I-Sight. The loop's objective is to explore the design space for maximum efficiency and/or minimum noise configurations. For each type of blade design, the loop is run three times with different objectives each time:

- First run: find the maximum efficiency achievable using the given set of data.
- Second run: find the minimum overall SWL achievable using the given set of data.
- Third run: multi-objective optimization; maximize the efficiency and minimize the overall SWL simultaneously. This run represents a compromise between efficiency and noise.

The runs are performed for the design target point of 2300 m^3/h, and the optimizer is free to explore the whole design space. The results of each run are reported in Table 3. The values are made dimensionless by dividing efficiency and overall SWL by reference values: 100% is the maximum efficiency and the minimum SWL achievable.

Fan C is the best in terms of efficiency regardless of the set of objectives followed by Fan A and then Fan B. By seeking a minimum noise configuration, the efficiency drops considerably for all fans, however, the gains in SWL are not the same for a similar efficiency drop. Fan B for instance emits roughly the same noise level (around 1 dB difference) for all the runs while Fan A and C have a larger variation in noise level between the first and the second runs (around 5 dB). All in all, the best efficiency costs around 1 dB compared to the minimum noise for Fan B and around 5 dB for Fan A and C.

Table 3 – Efficiency and overall SWL for each fan and each run of the optimization loop

	Efficiency (Dimensionless)			**Overall SWL (Dimensionless)**		
	Fan A	**Fan B**	**Fan C**	**Fan A**	**Fan B**	**Fan C**
Max Efficiency	95,5 %	91,3 %	100 %	110,7 %	106,7 %	102,5 %
Min Noise	82 %	75,1 %	87,1 %	105 %	105,2 %	100 %
Compromise between Max Efficiency & Min noise	94,9 %	91,2 %	94,9 %	109,1 %	106,7 %	100,1 %

CONCLUSIONS

Installation effects have been assessed for three types of fans. The fans provide the same pressure rise at the target operating point but have different blade loading distributions. The first is loaded near the bottom, the second is loaded near the tip, and the third is loaded close to the mid-span. The load distributions have been evaluated via RANS simulations, and the pressure rise with experimental data. Seventeen fan supports have also been designed and manufactured based on a NOLH parameter distribution and each fan is tested with all the supports in an anechoic chamber at several flow rates. All in all, the DOE provided acoustic data that cannot be obtained numerically in an industrial context mainly because of the important computational time required.

The results show that shifting the blade's load to the tip makes the fan less sensitive to its environment in terms of efficiency and noise. Minimum noise and maximum efficiency are not obtained for the same combination of parameters. And depending on the maximum blade load position, the compromise between acoustics and aerodynamics is more or less important.

Three Response Surface Models corresponding to each type of blade loading have also been constructed and included in an optimization loop. The design space was explored for maximum efficiency and minimum noise configurations. The results show that a compromise needs to be found between acoustics and aerodynamics by seeking minimum noise and maximum efficiency simultaneously. Thus, for a blade loaded at the bottom, the "compromise" configuration costs 0.2% efficiency and 1.3dB(A) compared to maximum efficiency or minimum noise configurations. For a blade loaded at tip, the best efficiency configuration is the best compromise. However, the results from the RSM need to be validated with experimental data, which will be the object of a future work.

ACKNOWLEDGMENT: This study was supported by the European project ECOQUEST – Seventh Framework Program, FP7 – SST – 2008 – RTD – 1.

BIBLIOGRAPHY

[1] S. Moreau, M. Roger - *Competing broadband noise mechanisms in low speed axial fans*- AIAA 2004-3039, **2004**

[2] T. Cioppa, - *Efficient nearly orthogonal and space filling experimental designs for high dimensional complex models*- September **2002**

[3] S. Moreau, M. Henner, - *Analysis of flow conditions in Freejet Experiments for studying Airfoil Self-Noise* -, AIAA Journal, Vol. 41, No. 10, October **2003**

[4] ISO 3744 - *Acoustics – Determination of sound power levels of noise sources using sound pressure – Engineering method for an essentially free field over a reflecting plane*- **1994**

[5] ISO DP 5801 – *Industrial Fans – performance testing using standardized airways*-, **1997**.